

Supplement of Atmos. Chem. Phys., 18, 16253–16269, 2018
<https://doi.org/10.5194/acp-18-16253-2018-supplement>
© Author(s) 2018. This work is distributed under
the Creative Commons Attribution 4.0 License.



Supplement of

Using CALIOP to constrain blowing snow emissions of sea salt aerosols over Arctic and Antarctic sea ice

Jiayue Huang et al.

Correspondence to: Lyatt Jaeglé (jaegle@uw.edu)

The copyright of individual parts of the supplement might differ from the CC BY 4.0 License.

1 Combining daytime and nighttime CALIOP observations to calculate nighttime-equivalent extinction coefficients

The daytime CALIOP estimates of aerosol extinction coefficients have higher sensitivity threshold than the nighttime estimates
5 due to the noise from solar photons (Winker et al., 2009), making nighttime extinction coefficients more accurate. Over polar
regions during summer, however, nighttime CALIOP observations are very limited due to constant solar illumination. In order
to examine the seasonal variation in CALIOP aerosol extinction coefficients over polar regions, we calculate nighttime-
equivalent CALIOP aerosol extinction coefficients following the approach of Di Pierro et al. (2013). The nighttime-equivalent
aerosol extinction is the weighted average of nighttime and adjusted daytime aerosol extinction coefficients. The daytime
10 aerosol extinction coefficients are adjusted with a scaling factor, which takes into account the different sampling frequency of
daytime and nighttime observations. The nighttime-equivalent aerosol extinction coefficient (ϵ_{neq}) is calculated following Eq.
(1):

$$\epsilon_{\text{neq}} = (f_n \cdot \epsilon_n \cdot N_n + f_d \cdot \text{SF} \cdot \epsilon_d' \cdot N_d) / (N_n + N_d), \quad (1)$$

where f is the aerosol detection frequency and the subscripts of d and n correspond to the daytime and nighttime. The ϵ
15 symbol denotes the observed aerosol extinction coefficient, and $\epsilon_d' = \epsilon_d / 1.6$, which is scaled to take into the account of higher
sensitivity threshold of daytime data (See following and Fig. S1a). SF is a scaling factor taking into account the different
detection sensitivities of daytime and nighttime retrievals. N is the number of CALIOP samplings.

In the absence of daytime data, we have

$$\epsilon_{\text{neq}} = f_n \cdot \epsilon_n \quad (2)$$

20 as we assign undetected aerosol layers (or clear air) an extinction coefficient value of 0.0 km^{-1} .

The scaling factor, SF, is defined as $\text{SF} = f_n / f_d$ based on the relationship between SF and backscatter coefficient during winter
months (November-April for the Arctic and May-October for the Antarctic) over the $62\text{-}70^\circ \text{ N/S}$ latitude band following Di
Pierro et al. (2013).

25 Figure S1c shows that both daytime and nighttime aerosol detection frequency decrease with height during Arctic ($62\text{-}70^\circ \text{ N}$)
winter (October-April 2007-2009), with the daytime detection frequency being 1.5-8 times lower than the nighttime detection

frequency. The average daytime aerosol backscatter coefficients are ~60% higher than the nighttime ones, as the daytime profiles have a higher sensitivity threshold and do not detect faint aerosol layers with lower aerosol extinction coefficients. Scaling the daytime aerosol backscatter coefficients by 0.6 ($\beta'_d = \beta_d / 1.6$) we get a daytime backscatter vertical profile in good agreement with the nighttime one (Figure S1b). A linear fit between the f_d / f_n and mean aerosol backscatter coefficient ($\beta =$
5 $[\beta_n + \beta'_d] / 2$), results in the following relationship between the scaling factor (SF) and β

$$SF = f_n / f_d = 1 / [0.123 + 0.148 \cdot \beta] \quad (3)$$

We combined equations (3) and (1) and get the estimate of nighttime equivalent data for the Arctic as shown in Fig. 3a–b. The monthly nighttime equivalent aerosol extinction coefficients agree with the nighttime one within 10% during winter (September–April). During May and July, the nighttime aerosol extinction is higher than the nighttime-equivalent one, as the
10 nighttime overpass only reach up to 62°N and over 60% of the 60–62°N band is covered by continents and generally has higher aerosol extinction than the central Arctic. The wintertime (November–April) vertical profile of nighttime-equivalent aerosol extinction agrees with the nighttime one within 5% (Fig. S3b).

We also derive the nighttime-equivalent scaling factor for the Antarctic in the same manner (Fig. S2), and get:

$$SF = 1 / [0.121 + 0.122 \cdot \beta] \quad (4)$$

15 The calculated nighttime-equivalent aerosol extinction coefficients in the Antarctic is in close agreement with the nighttime ones in February–November (Fig. S3c). The much higher nighttime aerosol extinction, in December–January, compared to the nighttime-equivalent, is again due to the limited nighttime overpass up to 62°S, and the zonal mean aerosol extinction coefficients decrease toward south pole over the Southern Ocean (Fig. 3). The wintertime (May–October) nighttime equivalent vertical profiles closely agree with the nighttime data (Fig. S3d).

20 **2 Calculating FYI and MYI in MERRA**

The multi-year sea ice (MYI) extent in this study is defined as the minimum sea ice extent during summer (September for Arctic and February in Antarctic) in the MERRA fields. In January–September over the Arctic, the MYI sea ice extent is the previous September minimum sea ice extent. We apply the same method for the Antarctic. We calculate the first-year sea ice (FYI) extent by subtracting the MYI extent from the MERRA total sea ice extent. Figure S4 shows the seasonal variations of
25 FYI and MYI sea ice extent over the Arctic and Antarctic.

3 Monthly maps of aerosol extinction coefficients

Fig. S5 and S6 show 2007-2009 mean monthly maps of the distribution of aerosol extinction coefficients over the Arctic and Antarctic for November through April (Arctic) and May through October (Antarctic). Monthly extinction coefficients from CALIOP are compared to those from the four GEOS-Chem simulations. Also shown in Fig. S5 and S6 are monthly FYI and MYI sea ice coverage. Overall, the monthly comparisons are consistent with the mean cold-season comparison (Fig. 1 and 4 in the main manuscript), with STD+Opt. Snow best capturing the spatial distributions of CALIOP aerosol extinction coefficients among four model simulations

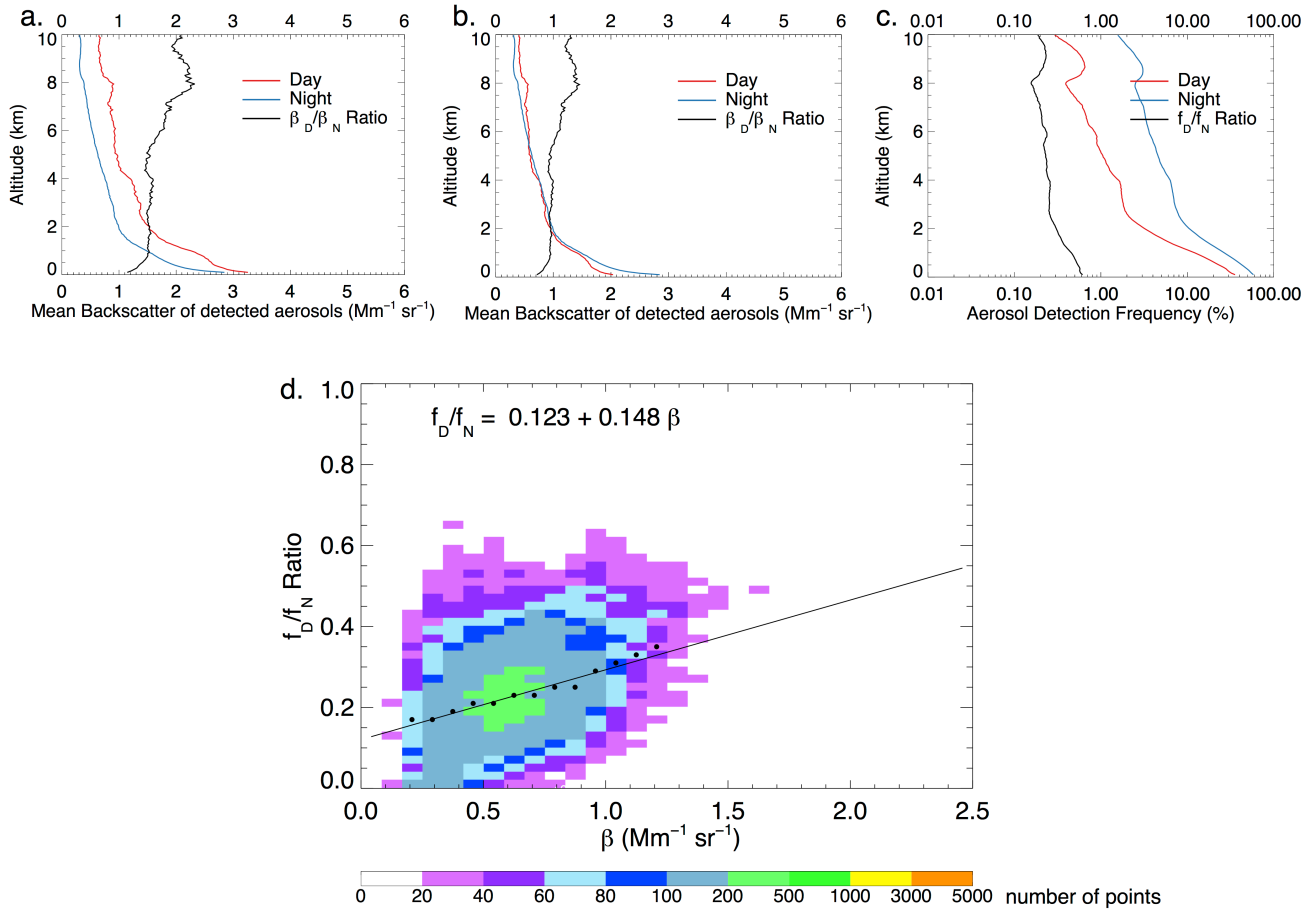
4 Sensitivity blowing snow simulations

We conduct two sensitivity simulations: 1) STD+Snow (N=1), which is the same as the STD+Snow simulation but assumes N=1 (number of SSA particle produced per snowflake) instead of N=5; 2) STD+Const. Snow, same as STD+Snow but applying a higher surface snow salinity on FYI over the Arctic (0.11 psu) and lower surface snow salinity on FYI over the Antarctic (0.018 psu). The choice of the FYI salinity was made to minimize the cold-months bias between GEOS-Chem and CALIOP. Results are shown in Fig. S7 for the Arctic and Fig. S8 for the Antarctic. Over the Arctic, the STD+Opt. Snow has best agreement with CALIOP among four blowing snow simulations. Over the Antarctic, the STD+Opt. Snow, STD+Snow (N=1) and STD+Const. Snow display similar model performances.

References

- Di Pierro, M., Jaeglé, L., Eloranta, E. W., and Sharma, S.: Spatial and seasonal distribution of Arctic aerosols observed by the CALIOP satellite instrument (2006–2012), *Atmos. Chem. Phys.*, 13, 7075-7095, <https://doi.org/10.5194/acp-13-7075-2013>, 2013.
- Winker, D. M., Vaughan, M. A., Omar, A., Hu, Y., and Powell, J. A.: Overview of the CALIPSO Mission and CALIOP Data Processing Algorithms, *J. Atmos. Ocean. Tech.*, 26, 2310–2323, doi:10.1175/2009JTECHA1281.1, 2009.

Arctic (62-70 N, 2007-2009)



5 **Figure S1:** Vertical profiles of backscatter coefficients for detected aerosol layers (a–b) and aerosol detection frequency (c) in November–April 2007–2009 at 62°–70°N. The daytime backscatter coefficients shown in (b) are scaled ($\beta'_D = \beta_D/1.6$). Daytime profiles are shown in red lines, and nighttime profiles are shown in blue lines. The black lines in a–b indicate the ratios of daytime-to-nighttime backscatter coefficients. The black line in (c) shows the ratios of daytime-to-nighttime aerosol detection frequency (f_D/f_N). Shown in (d) is the scatterplot of f_D/f_N ratio as a function of the mean backscatter coefficients. The colors represent the number of points in each bin. Black circles are the median f_D/f_N ratio for the corresponding mean backscatter coefficient. The black line is the linear fit of the black circles.

Antarctic (62-70 S, 2007-2009)

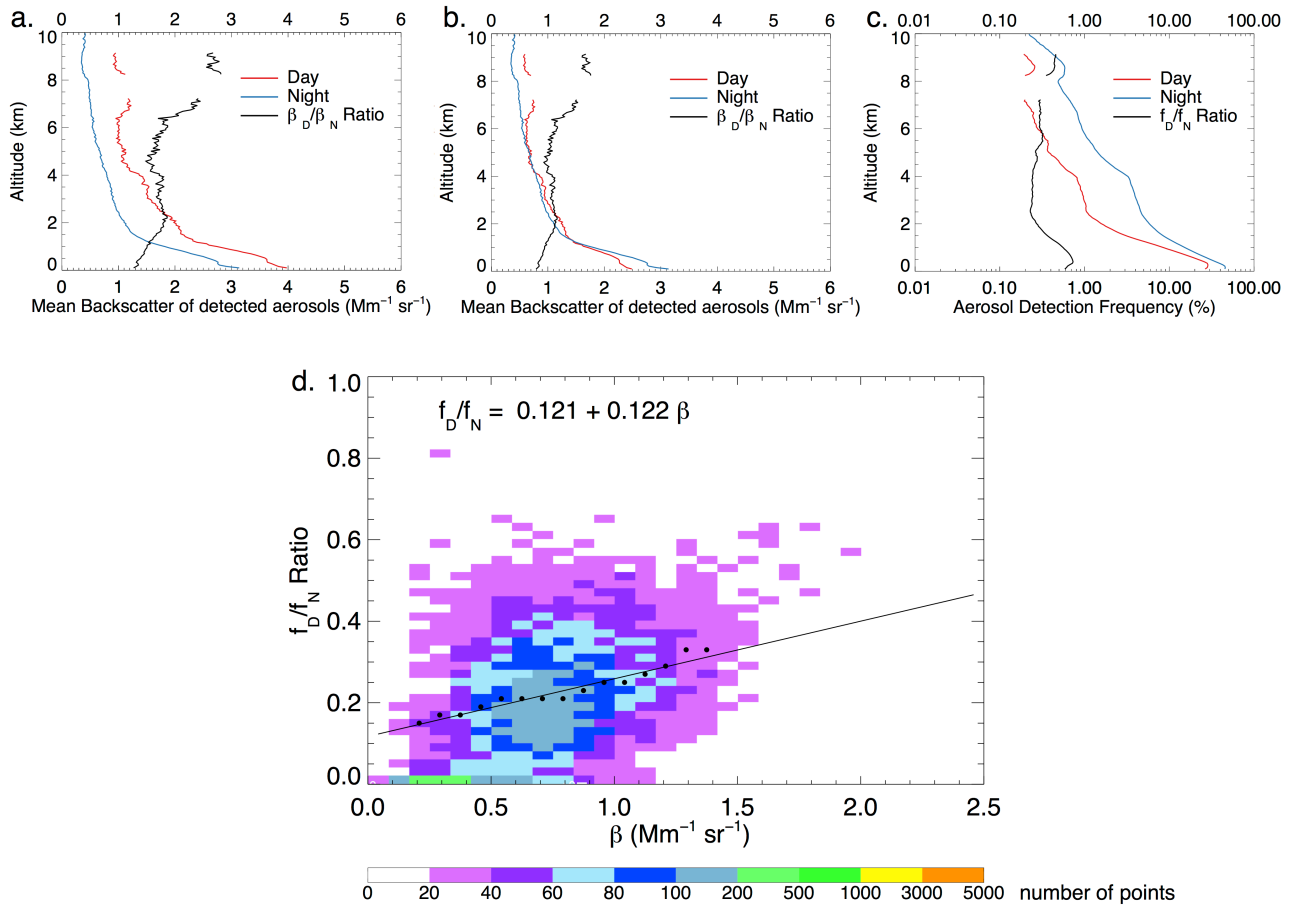
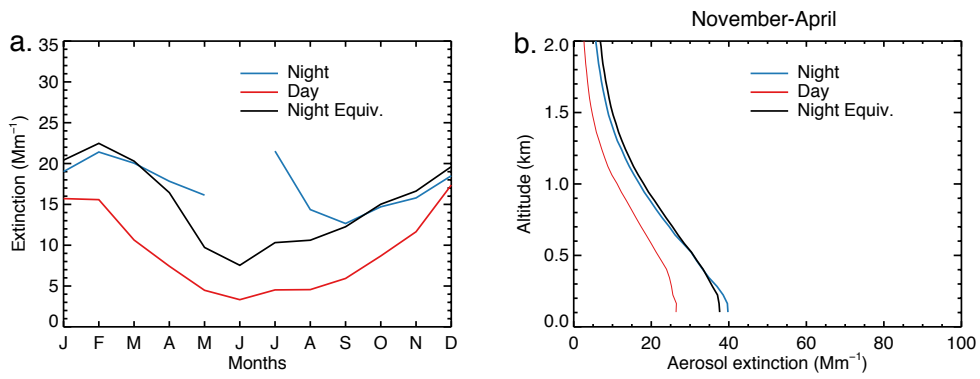


Figure S2: Same as Figure S1, but for May–October 2007-2009 at 62°–70°S.

Arctic (60-84 N, 2007-2009)



Antarctic (60-80 S, 2007-2009)

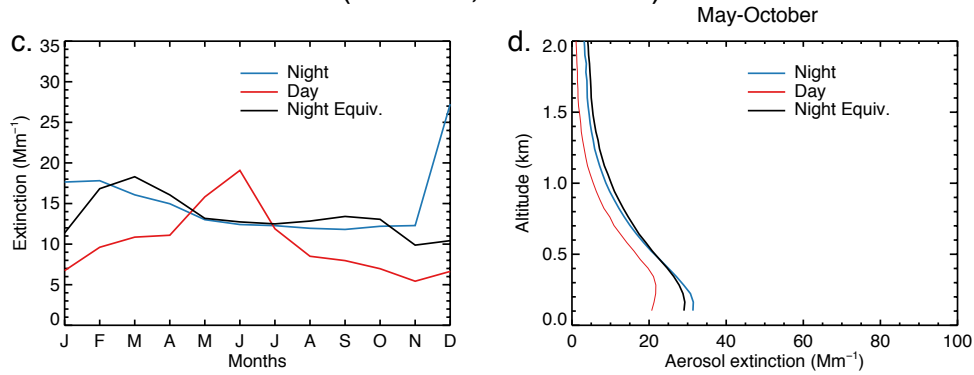


Figure S3: Comparison of seasonal variations of daytime, nighttime and nighttime-equivalent extinction coefficients over the (a) Arctic and (c) Antarctic. Also shown are the vertical profiles of daytime, nighttime and nighttime-equivalent extinction coefficients in the (b) Arctic winter (November–April) and (d) Antarctic winter (May–October).

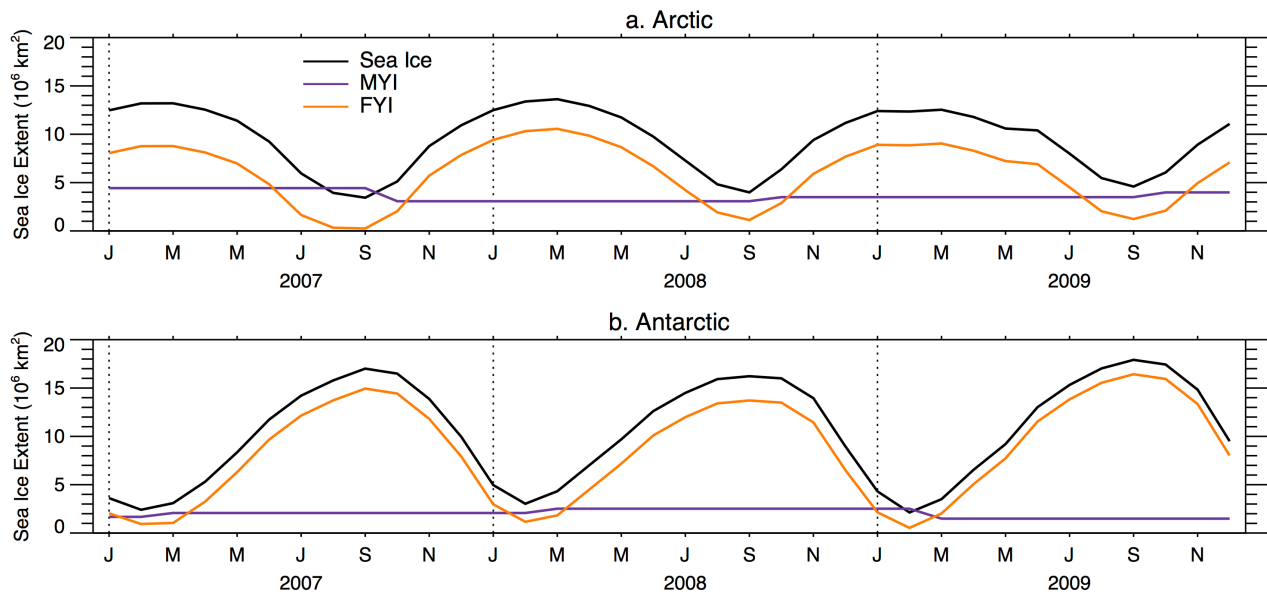


Figure S4: Seasonal variation of monthly sea ice extent (10^6 km^2) of total sea ice (black lines), first-year sea ice (FYI, orange lines) and multi-year sea ice (MYI, purple lines) over the (a) Arctic and (b) Antarctic.

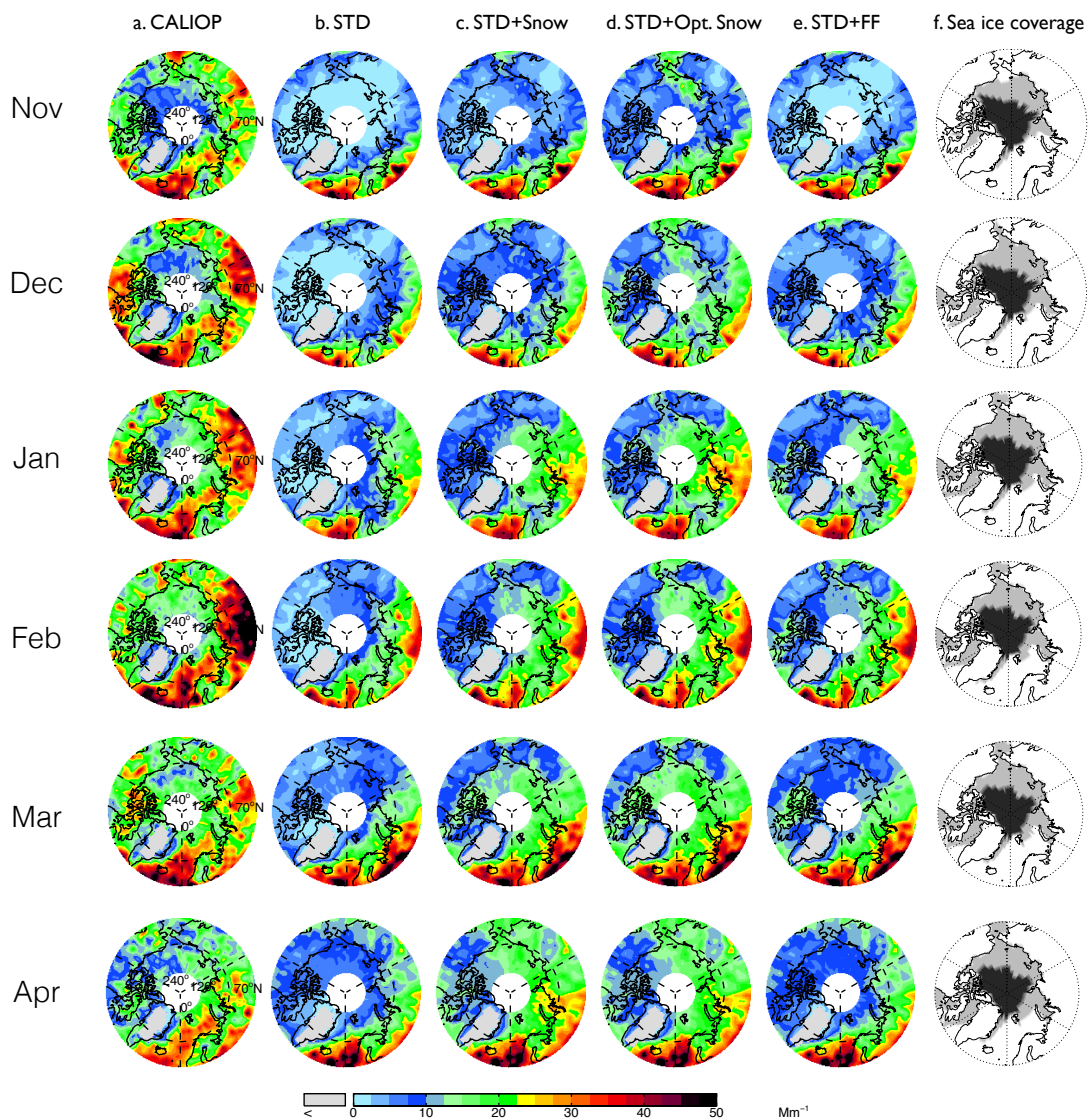


Figure S5: Monthly mean (2007-2009) spatial distribution of mean aerosol extinction coefficients (0–2 km) for November through April over the Arctic observed by (a) CALIOP and calculated with the GEOS-Chem model in (b) a Standard simulation (STD), (c) a simulation including blowing snow SSA emissions (STD+Snow), (d) an optimized blowing snow simulation (STD+Opt. Snow), and (e) a simulation including frost flower SSA emissions (STD+FF). The simulated extinction coefficients are sampled at the time and location of the CALIOP overpasses, and the CALIOP sensitivity threshold is applied. Also shown are the (f) monthly MERRA sea ice coverage, with light gray shading indicating FYI and black shading for MYI.

5

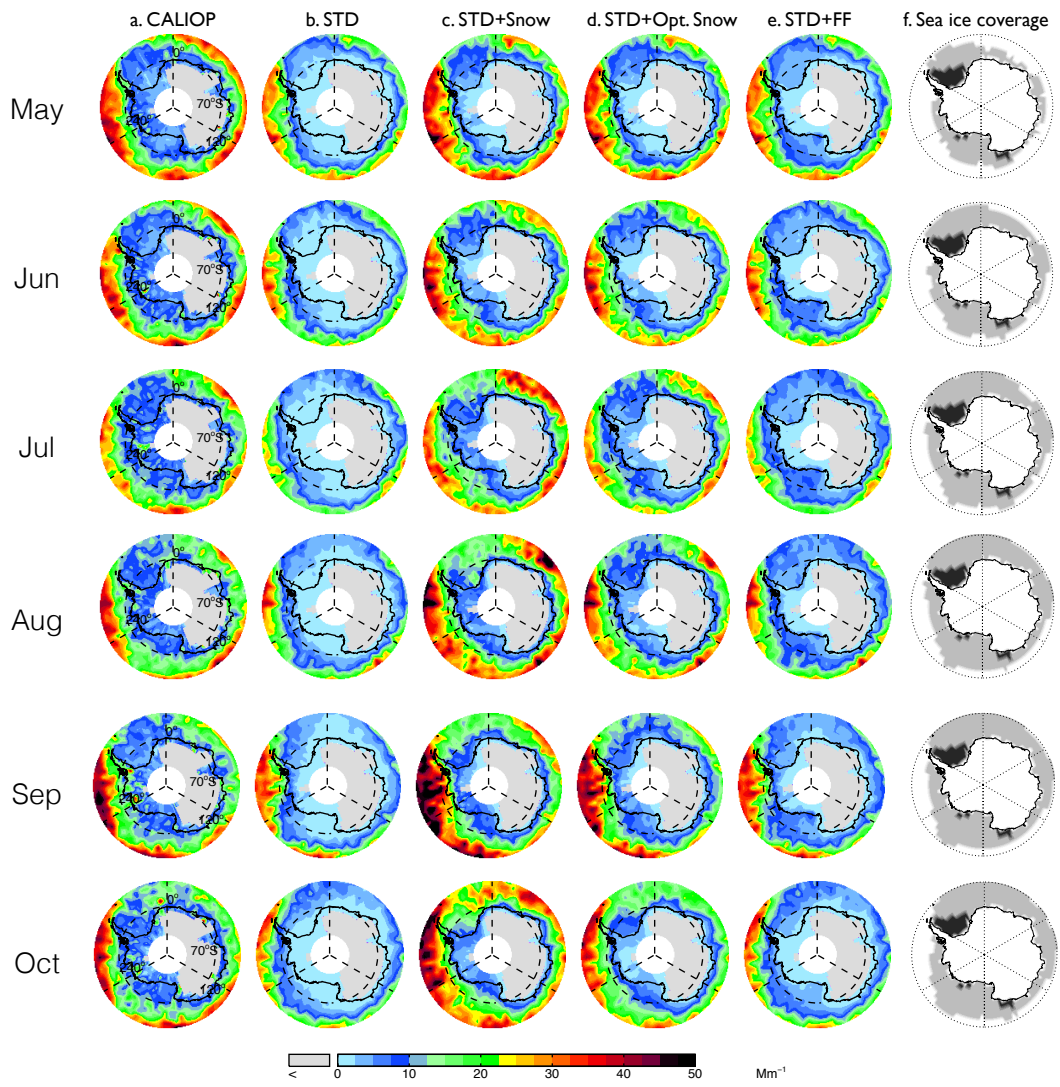


Figure S6: Same as Figure S5, but for Antarctic cold months (May–October)

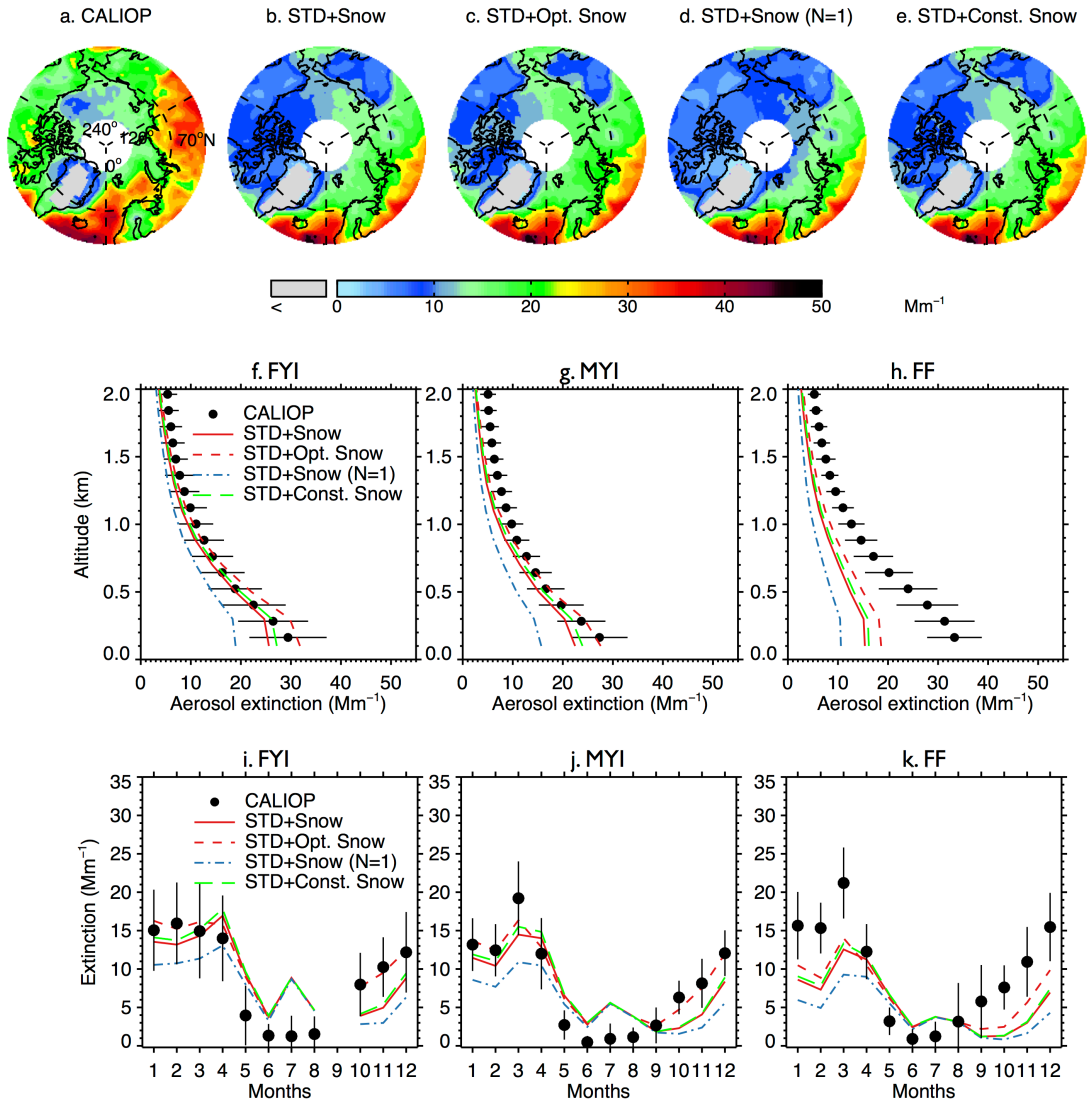


Figure S7: Cold season (November–April) spatial distribution of mean aerosol extinction coefficients (0–2 km) in the 2007–2009 over Arctic observed by (a) CALIOP and calculated with the GEOS-Chem model in (b) a simulation including blowing snow SSA emissions (STD+Snow), (c) an optimized blowing snow simulation (STD+Opt. Snow), (d) same as STD+Snow simulations but with number of particle produced per snowflake $N=1$ (STD+Snow ($N=1$)), and (e) same as STD+Snow simulations but applying a single scaling factor for surface snow salinity (STD+Const. Snow). Middle row: Vertical profiles of Arctic cold season mean aerosol extinction coefficients over (d) FYI, (e) MYI and (f) CAA for CALIOP (black dots with horizontal lines indicating standard deviations) and GEOS-Chem model simulations (STD+Snow: red solid lines, STD+Opt. Snow: red dashed lines; STD+Snow ($N=1$): blue dashed lines; STD+Const. Snow: green dashed lines). Bottom row: Seasonal cycle of 0–2 km monthly aerosol extinction coefficients averaged over (g) FYI, (h) MYI and (f) CAA. CALIOP observations are shown as black circles and vertical lines indicate the interannual standard deviation. The four GEOS-Chem model simulations are also shown (STD+Snow: red solid lines, STD+Opt. Snow: red dashed lines; STD+Snow ($N=1$): blue dashed lines; STD+Const. Snow: green dashed lines).

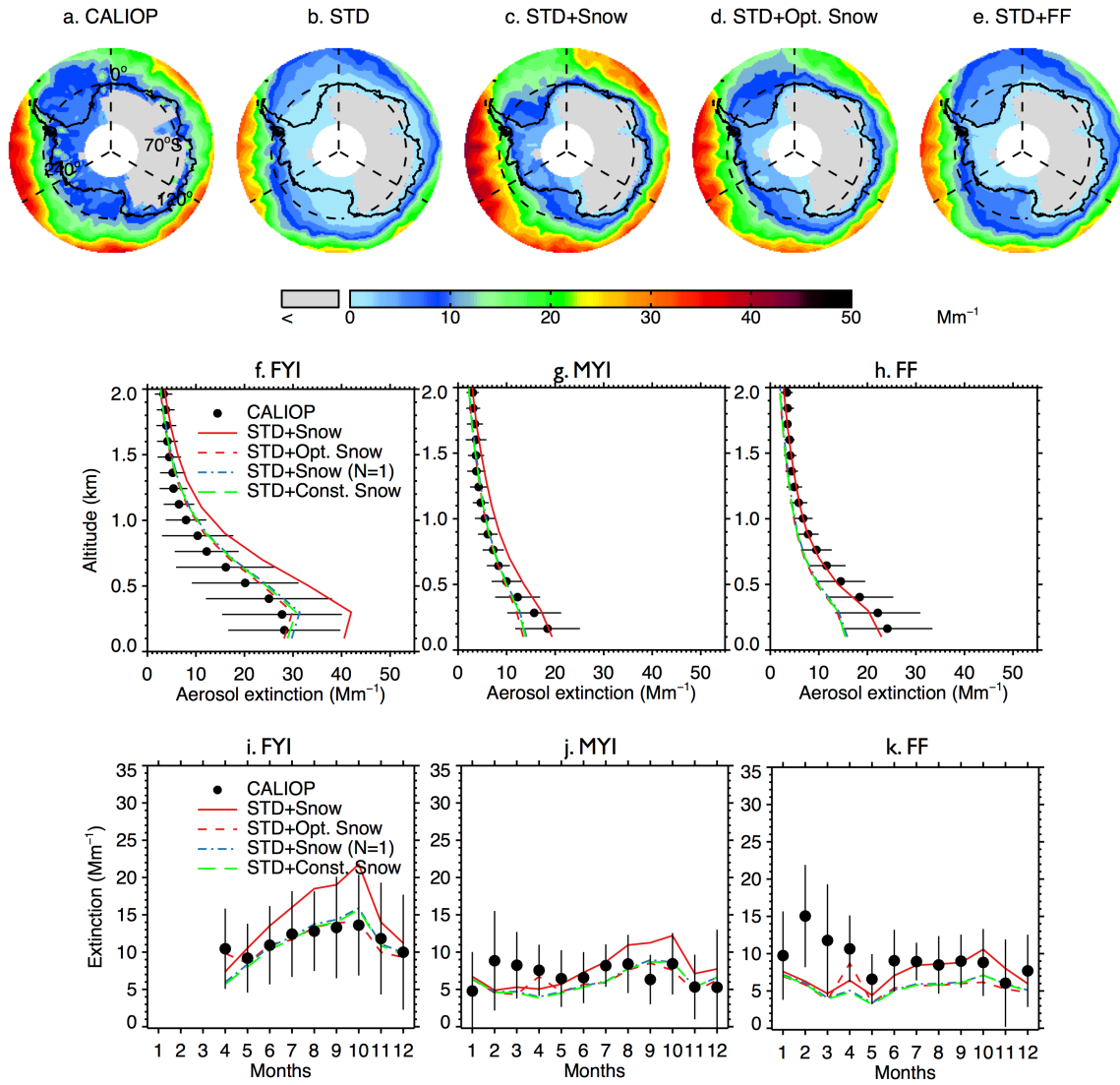


Figure S8: Same as Figure S7, but for the Antarctic aerosol extinction coefficients during Austral winter (May–October) over FYI (excluding offshore Ross Ice-shelf), MYI and offshore Ross Ice-shelf. As shown in (f), the monthly average aerosol extinction coefficients are not available over FYI during Antarctic summer (January–March) due to the limited FYI extent.